PERGAMON

International Journal of Heat and Mass Transfer 42 (1999) 2041–2051

International Journal of HEAT and MASS TRANSFER

Suppressing free convection from a flat plate with poor conductor ribs

I. Sezai*, A.A. Mohamad

Mechanical Engineering Department, Eastern Mediterranean University, North Cyprus, G. Magosa, Mersin 10, Turkey

Received 15 December 1997; in final form 21 August 1998

Abstract

An experimental and numerical analysis is performed to investigate the effect of attaching poor conducting ribs on a vertical heated flat plate. Accordingly, a test cell is constructed and a mathematical model is developed. The ribs are made of a poor conducting material (plexiglass). The present work is intended to study the suppression of free convection from a vertical plate with ribs attached on the surface. The effects of rib height to span ratio and Rayleigh number are investigated experimentally and numerically for air as the working fluid. It has been found that adding ribs on the surface can reduce the rate of free convection heat transfer by as much as 75% compared with a bare plate. Rather complex recirculatory flow patterns are predicted in the space between the ribs at high Rayleigh numbers.

Nomenclature

c specific heat
g gravitational acceleration
h heat transfer coefficient
H rib height
j unit vector along gravitational direction
k thermal conductivity
L_x width of solution domain
L_y height of the plate
N number of ribs
Nu Nusselt number, hL_y/k
p pressure
Ra Rayleigh number, $g\beta(T_1-T_2)L_y^3/\alpha v$
S rib spacing
t time
T temperature
u, v velocity components in x- and y-directions
x, y coordinate axes (see Fig. 1)
X, Y nondimensional coordinates, x/L_y and y/L_y respectively.

Greek symbols
α thermal diffusivity, $k/\rho c$
β thermal expansion coefficient
θ nondimensional temperature, $(T-T_c)/(T_h-T_c)$
μ dynamic viscosity
v kinematic viscosity, μ/ρ
ρ density.

Subscripts
ave average
c cold
h hot
i, j direction indicator
o bare plate.

1. Introduction

One of the methods of suppressing natural convection in storage tanks is to add ribs on the inner walls of the tank. The ribs restrict the fluid motion in the storage tank and accordingly decrease the rate of heat transfer. Also, in designing solar collectors without glass cover, there is a need to reduce convection heat transfer by free and forced convection. This type of solar collectors can be used for dual purposes; during daytime they can be used

* Corresponding author. Fax: 00 90 392 366 1217; e-mail: sezai@menet.me.emu.edu.tr

0017–9310/99/$ - see front matter
PII: S0017–9310(98)00305–6

for heating the working fluid, utilising solar energy and at night they can be used for cooling the fluid by infrared radiation exchange with the sky. It is necessary to reduce convective heat transfer from the absorber by suppressing air movement over the heated surface.

A literature survey shows that extensive work has been done on the enhancement of heat transfer by adding extended surfaces with high thermal conductivity on the heated surfaces for the purpose of cooling, as in electronic packages. In the area of solar energy collection, there are published works on the suppression of natural convection between absorber plate and glass cover by utilising honeycombs.

Edwards [1] determined the effect of inserting parallel vertical walls on the onset of convection in a cavity heated from below and cooled from above. It was found that the geometry, i.e. aspect ratio has significant effect on the onset of convection in cavities. Edwards' work has direct applications in solar collectors fitted with honeycombs. Buchberg et al. [2] reviewed methods that are used to suppress the cellular convection in solar collectors. Mostly, honeycomb structure is used between absorber and glass cover to suppress natural convection. For effective suppression, the honeycomb should have an optimum geometry. Arnold et al. [3] performed experiments on a solar collector fitted with rectangular honeycombs. It was found that for vertical orientation, there was no apparent effect of horizontal aspect ratio (width to plate spacing) of the honeycomb on heat transfer down to values of 0.5. For near-horizontal orientations, there is a marked effect of horizontal aspect ratio on heat transfer for values below unity. Hoogendoorn [4] reviewed and analyzed in more detail the conjugate effect of radiation, conduction and convection for honeycombs, i.e. for small aspect ratio enclosures. From our conducted survey, no work could be identified on suppression of heat transfer when low conductor ribs are attached on the heated plate. This work is motivated for the design of a sky cooling system. The effective sky tempeature is below zero degree (depending on humidity, dust, cloudiness) and can be used to cool circulated water through a flat plate at night time. Since, the ambient temperature is higher than sky temperature, there is a need to suppress heat convection from plate to ambient by adding thin, poor conductor ribs. From numerical calculations in this study it has been found that heat transfer by conduction through the low conducting ribs is less than 2.4% of the total heat transfer for Rayleigh numbers between 10^5 and 10^7 indicating that the radiation heat transfer on the rib surfaces, which is eventually conducted through the ribs, has a negligible effect on the total heat transfer to or from the plate surface. It can be said that poor conducting ribs on a surface merely act as convection suppressors. In radiative cooling applications the radiative cooling from the ribs will not contribute directly, but the cooling of the plate will be enhanced indirectly by the suppression of convection.

Accordingly, an experimental test cell is constructed for studying the suppression of natural convection when poor conductor ribs are attached on a surface. The temperature of the heated plate was fixed by recirculating water through a double-counter passage in the aluminium base fixed at the back of the copper plate. The plate is exposed to ambient conditions. Different rib span ratios (height/spacing) are investigated for different Rayleigh numbers. The heat flux distribution is measured along the plate length. A mathematical model is also developed for obtaining a detailed picture of the flow structure. The experimental data are used for evaluation of the predicted results. Fair agreement between experimental data and numerical predictions are obtained. The results show that adding ribs can reduce the rate of heat transfer by as much as 75% compared with that of a bare plate.

2. Experimental set-up

The plate with ribs attached on its surface is shown in Fig. 1a schematically. The heated plate is copper with width of 150 mm, length of 280 mm and thickness of 20 mm. Isothermal conditions on the heated plate are provided by recirculating distilled water through double-counter passage in the aluminium base plate. Plexiglass ribs 3 mm thick and of various heights are attached on the surface of the plate with various spacings in order to study the effect of ribs on the heat transfer rate. The ribs are held in place between two plexiglass sidewalls on which plastic guideways are glued. The surface of the heated plate is electroplated to minimize the radiation heat transfer. As a result the emissivity of the surface is estimated to be less than 0.05. Six, equally spaced thin film heat flux sensors (Omega) are mounted along the centerline of the plate surface to measure the heat transfer rate from the plate to the ambient air. Heat flux sensors consist of 40 junction thermopile bonded to either side of a polyimide film (Kapton) barrier and have a sensitivity of appoximately 2.0 μV W^{-1} m^{-2}. The thermal resistance of the sensors is 3.5×10^{-3}°C W^{-1} m^{-2} which results in a temperature drop of less than 2°C between the front surface and rear mounting surface of the sensors under the operating conditions of the experiment. The sensors are 0.23 mm thick 28.5 mm wide and 35.1 mm long and are mounted on the surface using a thin film of epoxy. To minimize radiation heat transfer the surfaces of the heat flux sensors are covered with thin aluminium foil. The test cell is thermally insulated from bottom and sides with 20 mm thick foam.

Temperature control in the test cell is achieved via a constant temperature bath circulator. The circulator provides bath temperature control of ±0.1°C. The test cell is mounted on a platform.

The data acquisation system is programmed to record data at a rate of 3 Hz over 30 s followed by a 4.5 min idle

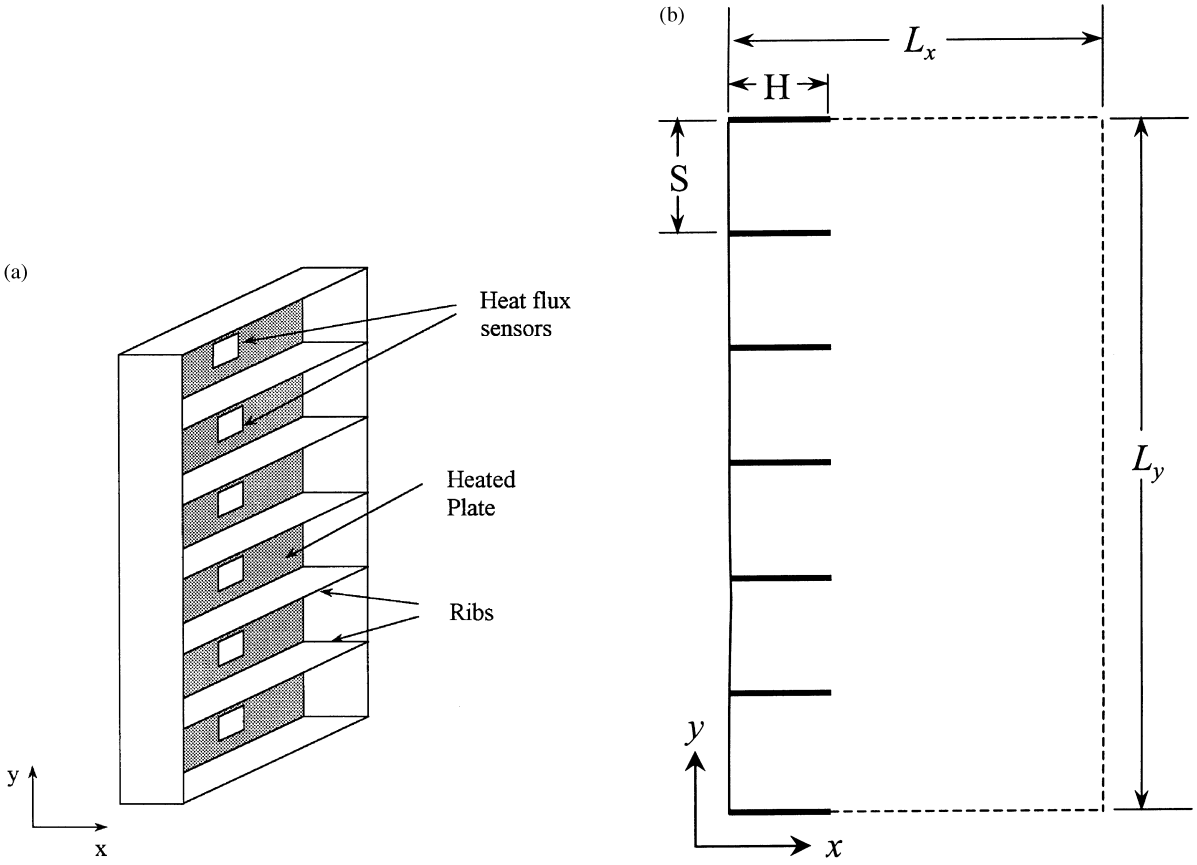

Fig. 1. Ribs for suppression of natural convection (a) schematic drawing and (b) computational domain.

period until 540 data are collected for each sensor for a single run. The recorded data is then averaged for the test run.

2.1. Calibration of heat flux sensors

The conversion factor for each individual heat flux sensor is supplied by the manufacturer. However, the calibration of the sensors may be altered when they are mounted on the surface of the heated plate via an epoxy film. Since the rate of heat transfer from a vertical heated plate is well established and the thermocouples used are accurately calibrated ($\pm 0.1^{\circ}C$), then the reading of the heat flux sensors for one experimental data are compared with the available correlations [5]. As a result, the conversion factors supplied by the manufacturer had to be adjusted slightly to match the correlated data which were also in close agreement with the numerical model predictions. The adjustment was done on the basis that the difference between the experimental and numerical predictions was observed systematically at different Rayleigh numbers.

Figure 2 shows the results for $Ra = 4.7 \times 10^7$ and 9.3×10^7 compared with well known correlations [5] and present numerical predictions. The temperatures of the plate and the surrounding air was 80 and 15°C, respectively, for $Ra = 9.3 \times 10^7$.

3. Mathematical formulation

3.1. Model equations

Consider laminar steady, two-dimensional flow and heat transfer over a heated, vertical plate with ribs attached on its surface (Fig. 1b). Assume that the flow is incompressible and thermophysical properties of the fluid are constant, except the density variation in the buoyancy term, i.e., Boussinesq approximation is valid. Continuity,

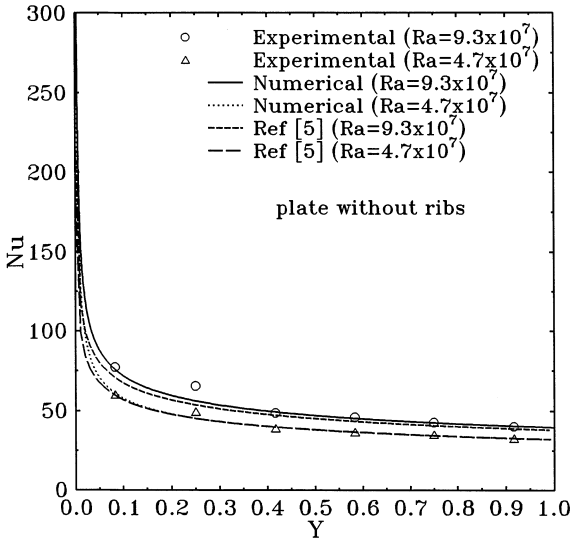

Fig. 2. Comparison of experimental data with numerical predictions for natural convection from a vertical flat plate without any ribs.

momentum and energy equations can be written as follows:

Continuity

$$\frac{\partial u_i}{\partial x_i} = 0 \tag{1}$$

Momentum

$$\frac{\partial \rho u_i}{\partial t} + \frac{\partial}{\partial x_j}(\rho u_j u_i) = -\frac{\partial P}{\partial x_i} + \frac{\partial}{\partial x_j}\left(\mu \frac{\partial u_i}{x_j}\right) + \rho g \beta (T - T_c)\mathbf{j} \tag{2}$$

Energy

$$\frac{\partial \rho c T}{\partial t} + \frac{\partial}{\partial x_j}(\rho c u_j T) = \frac{\partial}{\partial x_j}\left(k \frac{\partial T}{\partial x_j}\right) \tag{3}$$

In the above equations, ρ, μ, β, c, g and $\mathbf{j}$ stand for density, viscosity, thermal expansion coefficient, specific heat, gravity and unit vector along the gravitational direction, respectively.

3.2. Boundary conditions

The velocity components are set to zero at the solid boundaries and the vertical plate is kept at a higher temperature than ambient. Since, the flow field is not known prior to solution, the problem is solved over the domain extended in x-direction ($L_x = 0.55L_y$). The boundary conditions are treated as follows,

for $x = 0, u = \mathrm{v} = 0$ and $T = T_h$

for $x = L_x$, $p = \dfrac{\partial u}{\partial x} = \dfrac{\partial \mathrm{v}}{\partial x} = 0$ and $T = T_c$.

For $y = 0$ and $y = L_y$ and for $x < H$ the following boundary conditions are adopted

$$u = \mathrm{v} = 0 \text{ and } \frac{\partial T}{\partial y} = 0.$$

For $y = 0$ and $x > H$,

$$\frac{\partial u}{\partial y} = \frac{\partial \mathrm{v}}{\partial y} = 0, \quad T = T_c,$$

and for $y = L_y$ and $x > H$,

$$\frac{\partial u}{\partial y} = \frac{\partial \mathrm{v}}{\partial y} = \frac{\partial T}{\partial y} = 0$$

In the analysis the local Nusselt number is defined as

$$Nu = \left.\frac{\partial \theta}{\partial X}\right|_{X=0} \tag{4}$$

and the average Nusselt number as

$$Nu_{ave} = \int_0^1 Nu \, dY. \tag{5}$$

where $\theta = (T - T_c)/(T_h - T_c)$, $Y = y/L_y$ and $X = x/L_y$

3.3. Method of solution and grid independence

A control volume, finite-difference technique was used to solve the model equations with specified boundary conditions. SIMPLER algorithm [6] was employed to solve the equations in primitive variables.

The governing equations are converted to a system of algebraic equations through an appropriate integration over each control volume of the domain through finite-difference approximation. The algebraic equations are solved using a line-by-line iterative procedure. The method sweeps the domain of integration along the axes and uses the tridiagonal matrix inversion algorithm for solving the equations. Fully implicit Euler method is used to march the solution in time. Very large pseudo-time steps are used to obtain the final converged solution. The dependent variables (velocities and temperature) are underrelaxed by a factor of 0.8 or 0.7. Underrelaxing the temperature field decreases the rate of convergence. It is found that more than 1000 iterations are necessary to get convergent solution for most calculations. The criteria of convergence are to conserve mass, momentum and energy globally and locally, and to insure convergence of pre-selected dependent variables to a constant value.

The ribs are modeled by deactivating flow at rib cross sections, i.e. high viscosity (10^{10}) is adopted in the domain of ribs. Also, thermal conductivity of the ribs is set to be 10 times greater than the thermal conductivity of air. Large gradients of variables are expected in the boundary layer which may become extremely thin at high Rayleigh numbers. Hence, it is necessary to adopt a very fine grid mesh in the boundary layer and in the regions of large gradients. Very fine grids are used near the surface of the heated plate with grid spacing increasing exponentially away from plate along x-axis. Fine, grids are also used

along y-axis, where denser grids are adopted near bottom and top boundaries. In the analysis 151×251 nodes are used in the x- and y-directions, respectively. Grid independent results are insured and compared well with the well known correlation [5] for free convection along a heated vertical flat plate (Fig. 2).

4. Results and discussions

The effect of adding 1, 5 and 11 ribs (excluding the ribs added at bottom and top ends) of 5.0 cm high, with $S/H = 2.80$, 0.93 and 0.46, respectively, are shown in Fig. 3a–c where large variation of Nusselt number in the interrib space is observed for a Rayleigh number about 1×10^8. The variation of the Nusselt number on a vertical heated plate, with 5 ribs of 1.0 cm high ($S/H = 4.66$) is shown in Fig. 4. In these figures the experimental data and numerical predictions agree fairly well.

The large variation of local Nusselt number in the interrib space precludes an accurate calculation of the average Nusselt number over the entire plate using only the six local heat flux measurements. For this reason numerical simulation is used for constructing a more

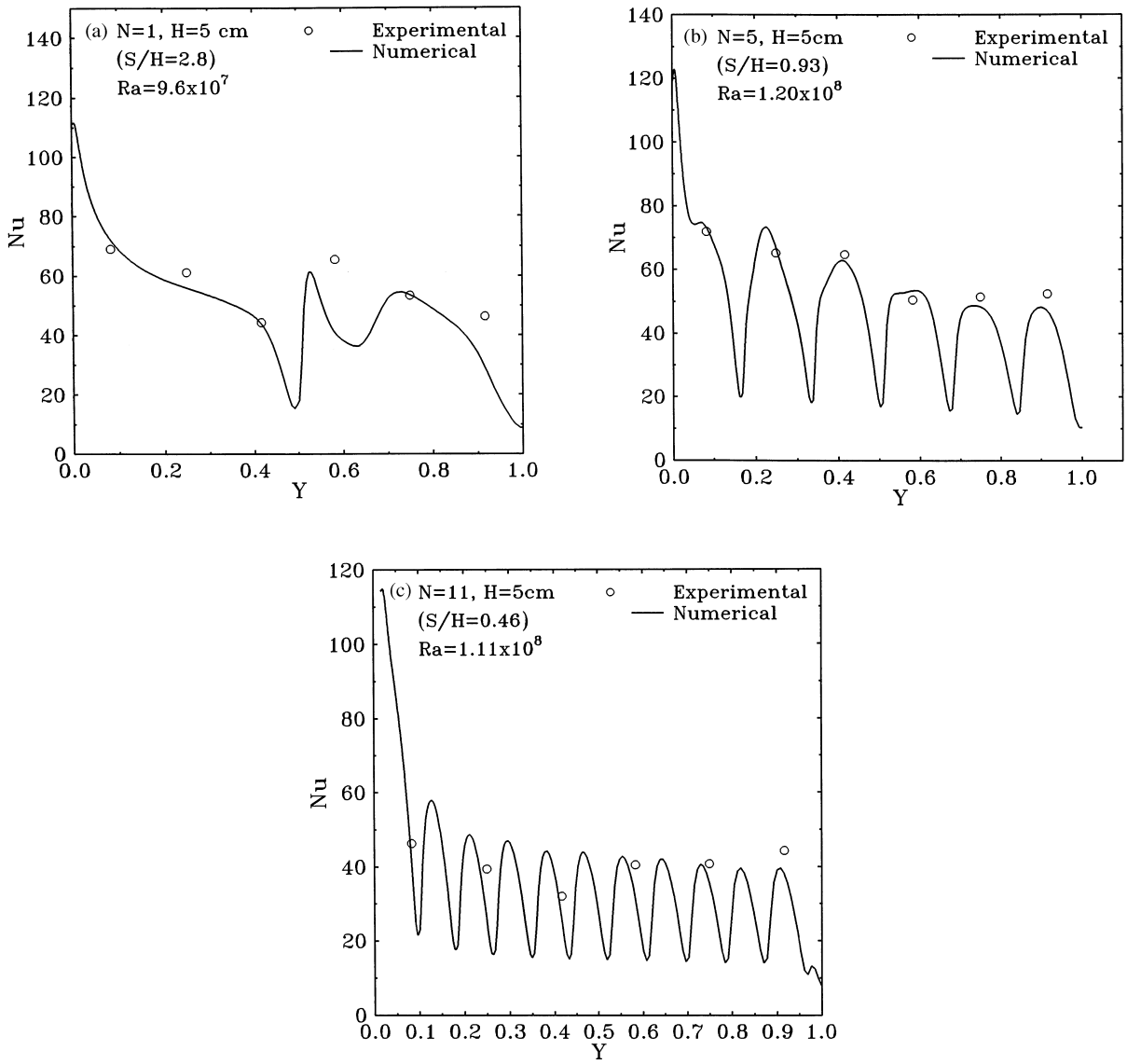

Fig. 3. Comparison of experimental data with numerical predictions for 5 cm high ribs attached on the surface. (a) $N = 1$, (b) $N = 5$, (c) $N = 11$.

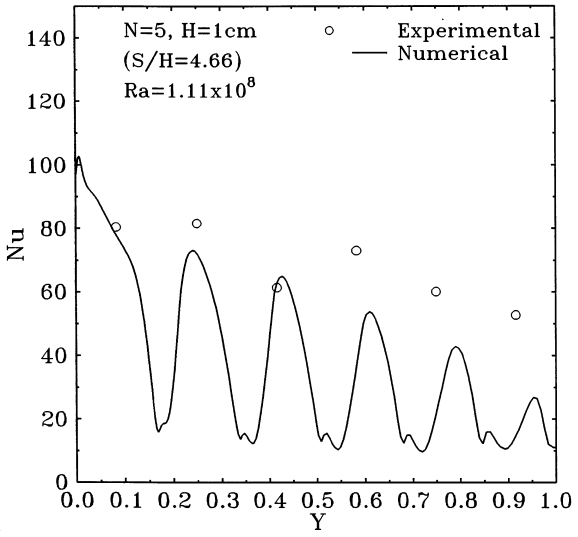

Fig. 4. Comparison of experimental data with numerical predictions for 1 cm high ribs attached on the surface.

detailed picture of the flow and heat transfer characteristics. The variation of the local Nusselt number with five 1.0 cm and 5.0 cm high ribs ($S/H = 4.66$ and 0.93) on the surface is compared with that of a plate without ribs ($H = 0$) in Fig. 5a and b for Rayleigh numbers of 10^5 and 10^7, respectively. For $Ra = 10^5$ (Fig. 5a) a reduction of natural convection heat transfer is obtained when ribs are attached on the surface. The reduction in heat transfer is as high as 50% for a rib height of 5.0 cm and $S/H = 0.93$. For 1.0 cm high ribs ($S/H = 4.66$), the reduction in Nusselt number is lower compared with that of 5.0 cm ribs. The variation in Nusselt number is periodic with maximum values attained at the middle of the inter-rib space and minimum values at the rib root. The amplitude of the variations is larger for 1.0 cm ribs compared with 5.0 cm. The amplitude of the Nusselt number variation is also found to increase with Rayleigh number. The decrease in Nusselt number resulting from attaching ribs on the plate surface is larger for 5.0 cm high ribs compared with 1 cm ribs for all Rayleigh numbers considered. A converged solution could not be obtained for 5.0 cm high ribs at $Ra = 10^8$.

The corresponding Nusselt number variations for 11 ribs on the plate are shown in Fig. 6a, and b for $Ra = 10^5$ and 10^7, respectively. The resulting rib span ratios S/H are 0.46 for 5.0 cm ribs and 2.33 for 1.0 cm ribs. From Figs 5 and 6 it can be observed that the amplitude of the Nusselt number variations decreases as the height and number of ribs increases, for all Rayleigh numbers considered. It can be concluded that decreasing the S/H ratio of the ribs on the surface decreases the amplitude of the Nusselt number variations on the plate. This is due to the fact that increasing the number and height of the ribs results in a restriction of the flow motion in between the ribs.

The average Nusselt number values over the entire vertical plate fitted with ribs are tabulated in Table 1, which include heat conduction from plate to the ribs. To find out the effect of heat conduction through ribs, the Nusselt number is also calculated by excluding the con-

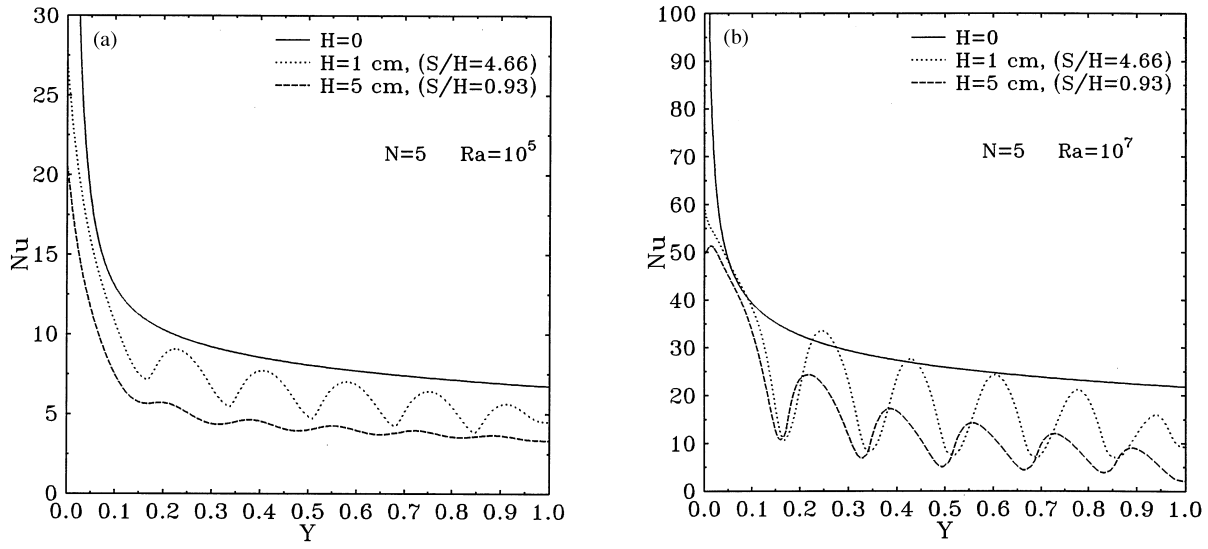

Fig. 5. Effect of widely spaced ribs on local Nusselt number for (a) $Ra = 10^5$ and (b) $Ra = 10^7$.

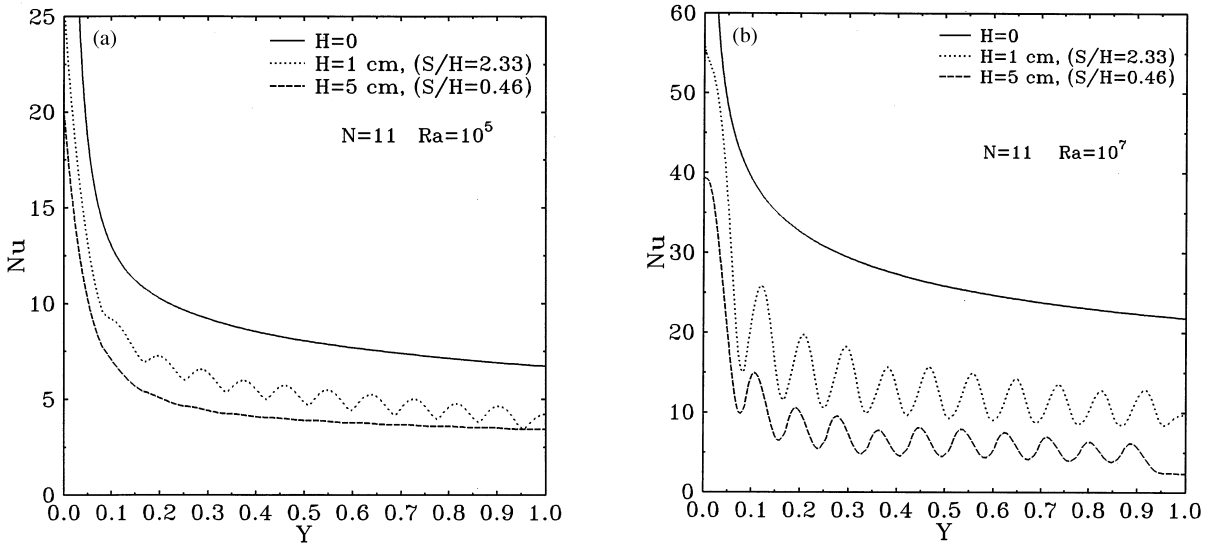

Fig. 6. Effect of closely spaced ribs on local Nusselt number for (a) $Ra = 10^5$ and (b) $Ra = 10^7$.

duction heat transfer through ribs. The difference between the two average Nusselt numbers is found to be less than 2.4% for all cases studied. Thus, it can be concluded that radiation heat transfer on the rib surfaces should have negligible effect on the average Nusselt number on the plate surface, since any heat transfer by radiation from rib surfaces is transferred by conduction from plate through ribs.

The ratio of average Nusselt number over the entire vertical plate fitted with ribs to that of a plate without ribs is shown in Fig. 7 as a function of rib spacing/rib height ratio for 1, 3 and 5 cm rib heights. The number of ribs considered are 3, 5, 7, 9 and 11 for each rib height. It can be noticed that the reduction of average Nusselt number, resulting from attaching ribs on the surface, increases as the S/H ratio of the ribs decreases. The suppression of average natural convection is as high as 75% for ribs with $S/H = 0.46$, for $10^5 \leqslant Ra \leqslant 10^7$. For $Ra > 10^6$ the average nusselt number is a function of rib height as well as the span ratio. Higher suppression of natural convection is achieved by using shorter rib heights for the same S/H.

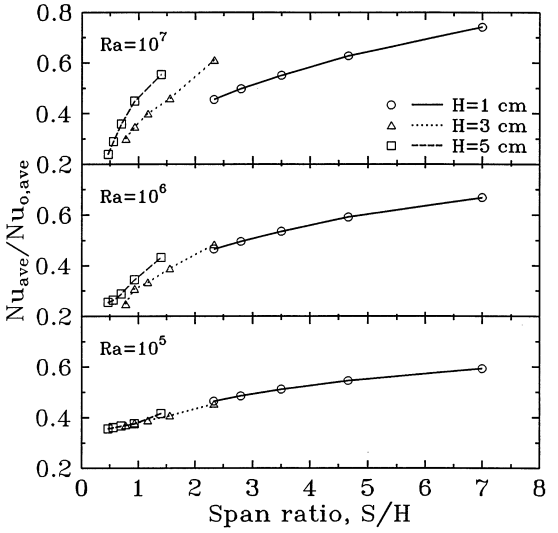

Fig. 7. Reduction of average Nusselt number on the plate surface fitted with ribs.

More insight on the heat transfer characteristics of ribbed surface can be obtained by examining the induced flow configurations. Figure 8a and b presents the flow patterns resulting from installing 5.0 cm high 11 ribs ($S/H = 0.46$) on the vertical plate for Rayleigh numbers of 10^5 and 10^7. For $Ra = 10^5$ the flow smoothly contours the walls of the cavities formed by the ribs at the bottom, with air flowing in from downstream and leaving at the upstream rib of each cavity. After the fourth rib, circulating flows composed of two oppositely rotating vortices are observed between the ribs. This explains why the Nusselt Number decreases along the plate with ribs. At $Ra = 10^7$ a single vortical flow occupies almost the whole interrib space and a small circulatory flow appears directly behind the tip of the ribs (Fig. 8b). As a result of the deceleration effects of the rather low S/H ratio ribs, high rate of suppression of natural convection results as depicted in Fig. 6a and b.

Table 1
Average Nusselt number on the plate

Rib height [cm]	Number of ribs	S/H	Nu_{ave}		
			$Ra = 10^5$	$Ra = 10^6$	$Ra = 10^7$
1.0	3	7.00	7.982	13.657	24.415
	5	4.66	7.393	12.096	20.693
	7	3.50	6.931	10.948	18.129
	9	2.80	6.576	10.134	16.380
	11	2.33	6.289	9.513	15.008
3.0	3	2.33	6.118	9.890	20.118
	5	1.55	5.490	7.948	15.142
	7	1.16	5.233	6.826	13.165
	9	0.93	5.081	6.288	11.446
	11	0.77	4.156	5.067	9.869
5.0	3	1.40	5.610	8.833	18.255
	5	0.93	5.097	7.021	14.793
	7	0.70	4.964	5.875	11.806
	9	0.56	4.889	5.399	9.509
	11	0.46	4.827	5.200	7.840
Bare plate			13.538	20.424	32.918

The flow structure for more widely spaced 5.0 cm ribs ($S/H = 0.93$) is shown in Fig. 9a and b for $Ra = 10^5$ and 10^7 respectively. For $Ra = 10^5$ the air flows smoothly, contouring the cavities formed by the ribs with no recirculation in between, except the two cavities at the top. The relatively uniform flow velocity results in a rather uniform heat transfer from the plate surface as depicted in Fig. 5a. At $Ra = 10^7$ a recirculating flow structure is formed in the interrib spaces after the first rib, counted from bottom (Fig. 9b). A small separation zone is also formed directly behind the tip of each rib. The heat transfer rate is maximum at the center of the cavities formed by the ribs and minimum near the ribs as depicted from Fig. 5b. Figure 10 shows the streamlines resulting from natural convection when 11 ribs, each having 1.0 cm height, are attached on the surface of the vertical plate for $Ra = 10^7$. The resulting span ratio S/H is 2.33. A vortex flow zone is formed directly behind the ribs, starting from the second rib. In the interrib spaces, a small stagnation zone is formed in the region directly attaching to the upper ribs.

When the span ratio S/H of 1.0 cm high ribs is increased to 4.66 a rather smooth, parallel flow is set up near the plate surface, except near a small region directly behind the ribs (Fig. 11) for $Ra = 10^7$. The resulting reduction in Nusselt number is small as depicted in Fig. 5b.

5. Conclusions

In the process of natural convection from a vertical heated plate, in the presence of poor conducting ribs attached on the surface, a reduction in heat transfer is observed due to the decelerating effect of the ribs for $Ra = 10^5$–10^7. This reduction is proportional to rib spacing/rib height (S/H) ratio, with higher reduction in Nu being obtained at smaller S/H ratios. For $S/H = 0.46$ and 4.66 the reduction in Nusselt number is 80 and 40%, respectively, compared with a bare plate. Nusselt number is maximum at the center of the region formed by the two consecutive ribs and minimum near the ribs. The amplitude of the Nusselt number variations decreases as S/H ratio is increased.

It has been found that heat transfer by conduction through the poor conducting ribs is less than 2.4% of the total heat transfer for the cases studied, indicating that radiation heat transfer on the rib surfaces, which is conducted through ribs, has negligible effect on the average Nusselt number on the plate surface.

A vortex motion is set up in the regions behind the ribs. The vortical air flow occupies the entire zone between the ribs as the Rayleigh number is increased. As the ratio of the rib height to rib width is increased the recirculatory zone occupies a larger fraction of the space between two consecutive ribs.

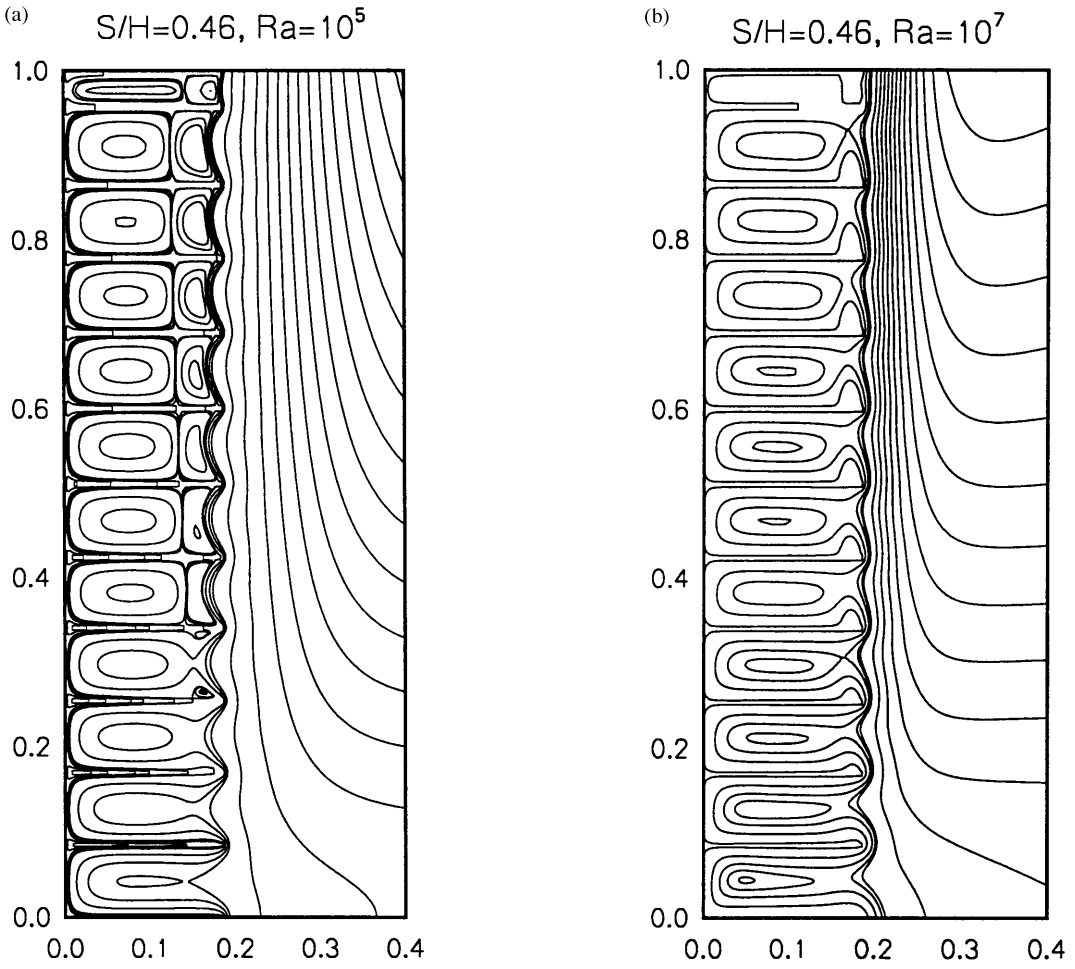

Fig. 8. Flow patterns resulting from attaching ribs with $S/H = 0.46$ on the surface for (a) $Ra = 10^5$ and (b) $Ra = 10^7$.

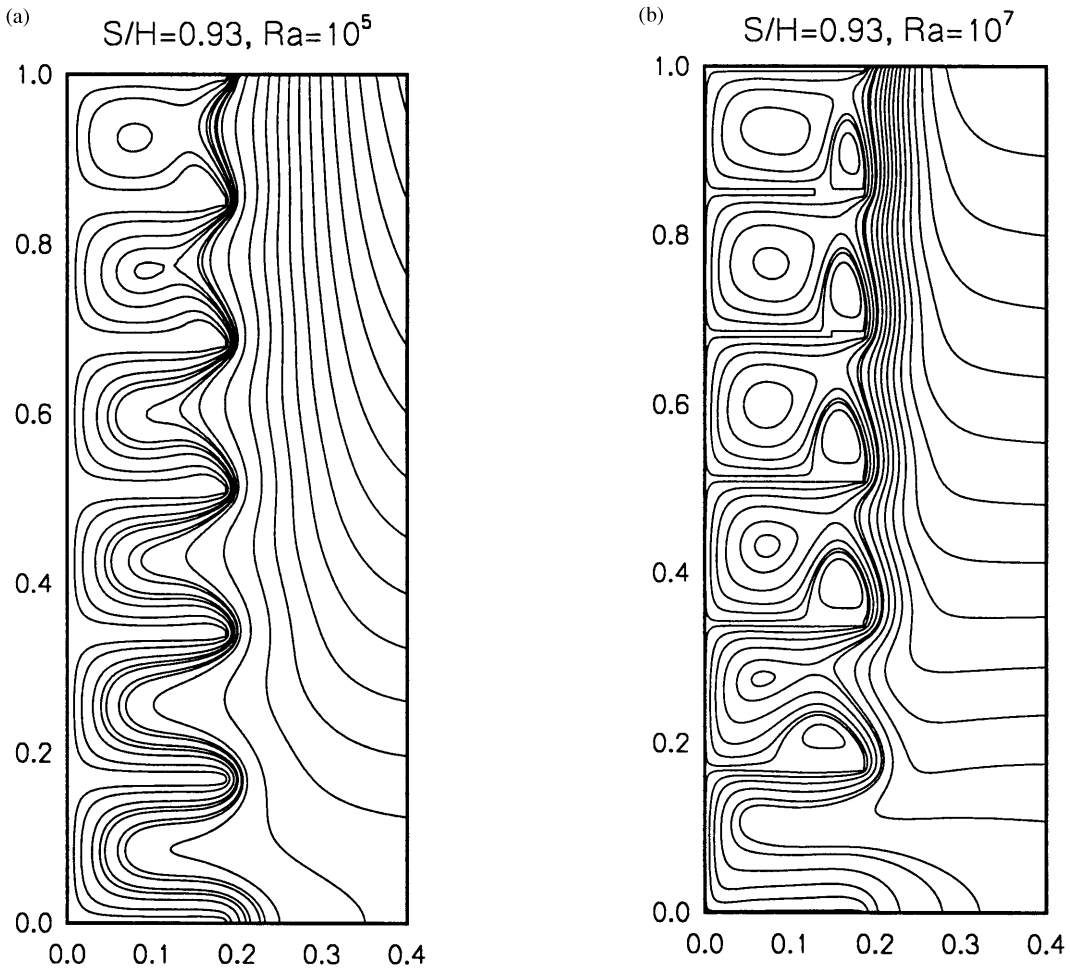

Fig. 9. Flow patterns resulting from attaching ribs with $S/H = 0.93$ on the surface for (a) $Ra = 10^5$ and (b) $Ra = 10^7$.

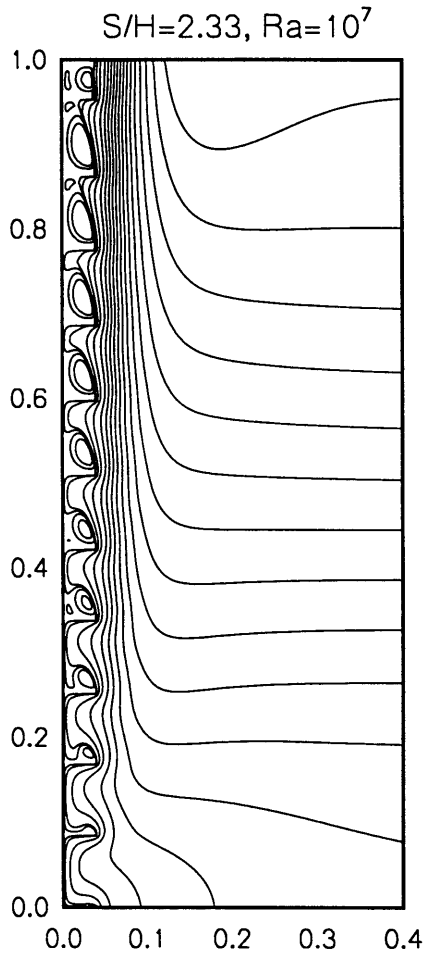

Fig. 10. Flow patterns resulting from attaching ribs with $S/H = 2.33$ on the surface for $Ra = 10^7$.

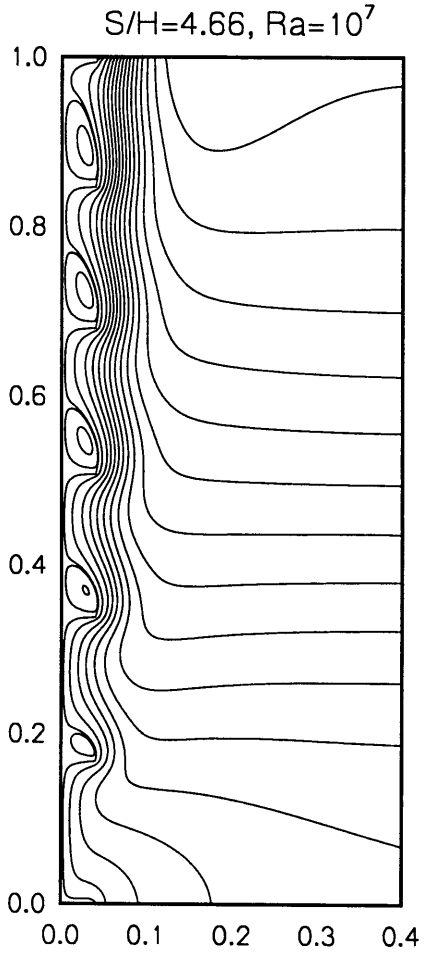

Fig. 11. Flow patterns resulting from attaching ribs with $S/H = 4.66$ on the surface for $Ra = 10^7$.

References

[1] D.K. Edwards, Suppression of cellular convection by lateral walls, J. Heat Transfer 91 (1969) 145–150.
[2] H. Buchberg, I. Catton, D.K. Edwards, Natural convection in enclosed spaces—a review of application to solar energy collection, J. Heat Transfer 98 (1976) 182–188.
[3] J.N. Arnold, D.K. Edwards, I. Catton, Effect of tilt and horizontal aspect ratio on natural convection in a rectangular honeycomb, J. Heat Transfer 99 (1977) 120–122.
[4] C.J. Hoogendoorn, Natural convection suppression in solar collectors, in: S. Kakac, W. Aung, R. Viskanta, (Eds.), Natural Convection, Fundamentals and Applications, Hemisphere Publishing Corp., New York, 1985, 940–960.
[5] F.P. Incropera, D.P. Dewitt, Fundamentals of Heat and Mass Transfer, Wiley, 1990.
[6] S.V. Patankar, Numerical Heat Transfer and Fluid Flow, Hemisphere, New York, 1980.